P26

DNA, π, and the Bell

Whether nature's complexity may be understood via deterministic mechanisms is a long-standing question in science. This work shows, through a simple procedure consisting of iterations of two or more suitable mappings, yielding space-filling fractal functions, that the peculiar rosette structure of life's DNA (and others) can be closely approximated as a mathematical design(s) embedded in a circular bivariate Gaussian distribution. This article expounds an intriguing hidden order in the digits of π, as iterations of two mappings according to the binary expansion of π are shown to yield a topologically correct representation of life's DNA rosette inside the bell.

CARLOS E. PUENTE

Carlos E. Puente is with the Department of Land, Air, and Water Resources and the Institute of Theoretical Dynamics, University of California, Davis, California 95616. He holds Master of Science degrees in Operations Research and Civil Engineering and a Ph.D. in Hydrology from MIT. He has been a faculty member at the University of California, Davis since 1986. His research is concerned with the geometric modeling of complexity, as encountered in geophysics and biology.

INTRODUCTION

With the advent of X-ray technology since last century, the remarkable structure of life's most relevant building blocks is being revealed. These developments have led to the discovery of beautiful arrangements, often times containing nontrivial symmetries, which make up the fabric of biochemistry, e.g., Voet and Voet [1]. The present work presents an unexpected connection between the two-dimensional rosette structure of life's DNA (and other natural patterns) and recently discovered mathematical designs that decompose bivariate Gaussian distributions [2]. This article also shows that the circular bell contains the topological structure of life's DNA rosette, when two simple affine mappings are iterated following the binary expansion of the number π. These results add to the vision that simplicity may be at the root of complexity and suggest that the bell may be of relevance not only in mathematics and physics but also in biology and chemistry.

The mathematical developments herein stem from new constructions of Gaussian distributions over one and two dimensions as discovered by Puente [3] and Puente and Klebanoff [4]. Under these formulations, Gaussian variates are obtained as projections of arbitrary diffuse measures (i.e., those having continuous cumulative distributions) supported by the graphs of plane- or space-filling fractal interpolating functions [5,6].

The organization of this work is as follows. First, the construction of bivariate Gaussian distributions is explained, followed by a brief account of the induced decompositions of circular bells. Then, an approximation of life's DNA rosette as a mathematical design inside the bell is given and the possible connection between DNA, π, and the bell is explained. Finally, conclusions and pertinent unsolved questions are presented.

THE BIVARIATE GAUSSIAN DISTRIBUTION AS A PROJECTION

The graph of a fractal interpolating function passing by $N + 1$ nonaligned data points in a three-dimensional space ($N \geq 2$), $\{(x_n, y_n, z_n): z_0 < \cdots < z_N\}$, is defined as the unique attractor of N affine mappings [6]:

$$w_n\begin{pmatrix} x \\ y \\ z \end{pmatrix} = \begin{pmatrix} a_n & b_n & c_n \\ d_n & e_n & f_n \\ 0 & 0 & g_n \end{pmatrix}\begin{pmatrix} x \\ y \\ z \end{pmatrix} + \begin{pmatrix} h_n \\ i_n \\ j_n \end{pmatrix}, \quad (1)$$

subject to

$$w_n\begin{pmatrix} x_0 \\ y_0 \\ z_0 \end{pmatrix} = \begin{pmatrix} x_{n-1} \\ y_{n-1} \\ z_{n-1} \end{pmatrix} \quad (2)$$

and

$$w_n\begin{pmatrix} x_N \\ y_N \\ z_N \end{pmatrix} = \begin{pmatrix} x_n \\ y_n \\ z_n \end{pmatrix}. \quad (3)$$

These conditions allow computing the coefficients c_n, f_n, g_n, h_n, i_n, and j_n, in terms of the data points and the free parameter matrix

$$A_n = \begin{pmatrix} a_n & b_n \\ d_n & e_n \end{pmatrix} \stackrel{\text{def}}{=} \begin{pmatrix} r_n^{(1)} \cos \theta_n^{(1)} & -r_n^{(2)} \sin \theta_n^{(2)} \\ r_n^{(1)} \sin \theta_n^{(1)} & r_n^{(2)} \cos \theta_n^{(2)} \end{pmatrix}, \quad (4)$$

where $r_n^{(i)}$ and $\theta_n^{(i)}$ are the *scalings* and *rotations* of the affine mappings.

This setting defines a unique function from the line (z) to the plane (x, y), which interpolates the initial set of data points and whose graph possesses a fractal dimension between one and three [6]. Such a graph may be obtained by progressively iterating the mappings w_n in great many ways, for instance, by using them randomly in succession, independently from time to time, and proportionally to prespecified (and possibly noneven) iteration frequencies p_n, $\sum_{n=1}^{N} p_n = 1$ [7]. Even though any such iteration scheme ultimately leads to the same *deterministic* graph, alternative iteration paths, filling-up the attractor in varying orders, define a vast variety of stationary diffuse measures (textures) over the same graph [8].

Figure 1 illustrates how to construct projections of such stationary measures over the (x, y) plane, for two sets of fractal interpolating functions that only vary in their scaling parameters. As is seen on the left, a fractal interpolating function with graph shaped as a convoluted *"wire"* (top) yields a stationary bivariate measure over the horizontal (bottom), when a histogram of acquired points in the function above is made over the (x, y) plane. As shown on the right, when the fractal interpolating function tends to fill up space (top), a bivariate Gaussian histogram appears (bottom). For the example shown, only a small portion of the points used to get a (circular) Gaussian histogram is plotted, but as may be seen, they land on an extremely large wire, which becomes unbounded as it fills up three-dimensional space.

Both wires on Figure 1 are obtained via independent iteration paths based on fair coin tosses, such that their two suitable affine mappings (with outcomes colored blue and red) are employed 50% of the time each. Because this iteration scheme yields uniform textures over both attractors [3], the

FIGURE 1

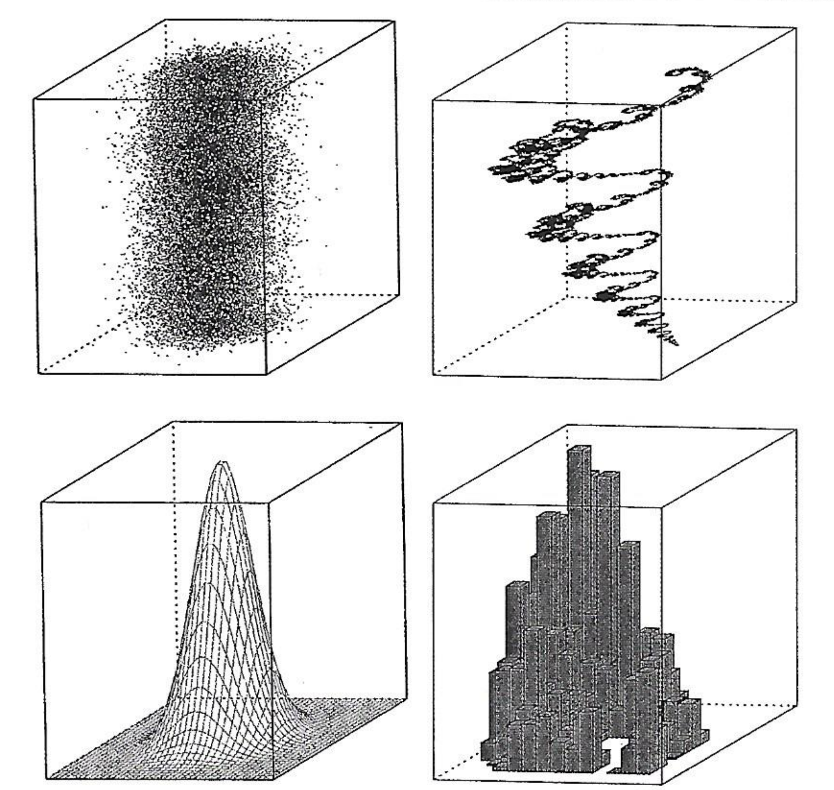

Fractal interpolating functions and horizontal projections. Data: $\{(0, 0, 0), (1, 1, \frac{1}{2}), (0, 0, 1)\}$. Rotations: $\theta_1^{(1)} = \theta_1^{(2)} = 0$, $\theta_2^{(1)} = \theta_2^{(2)} = \pi/3$. Scalings: $r = r_1^{(1)} = r_1^{(2)} = r_2^{(1)} = r_2^{(2)}$, left: $r = 0.70$, right: $r = 0.999$. The affine maps involved were iterated according to fair coin tosses. The colors correspond to their respective outcomes.

wire on the right illustrates that a bivariate bell is the limiting projection of a uniform measure supported by a fractal interpolating function, when such wire's fractal dimension tends toward three [4].

When biased coins are used to define other independent iteration paths, the same attractor now supports nonuniform diffuse measures having a multifractal character, e.g. Mandelbrot [9]. As it may be expected, different (horizontal) projections are now encountered on both wires in Figure 1, but, surprisingly, the space-filling case yields bivariate Gaussian distributions, irrespective of the chosen iteration frequencies [3,8]. The construction turns out to be *universal* as bells, with or without correlations [3,4], are encountered irrespective of the coin bias (p_n) and also for arbitrary diffuse measures defined over the wire. This includes arbitrary singular measures, which, despite having distributions that are devil's staircases (e.g., Feder [10]), are transformed into (different) bells by the same space-filling wire [4,8]. This remarkable result implies that space-filling fractal interpolating functions are "intrinsically Gaussian" objects, whose projections transform a vast class of measures (excluding only those having discrete jumps) into the harmonious bell.

Further insight into the construction via iterations is gained by also computing vertical projections of the stationary measures supported by the unique wires. Such projections define diffuse multifractal measures over the attractor's domain, $[z_0, z_N]$ and represent an underlying parent texture that is functionally *transformed* by the fractal interpolating function into the bivariate stationary measures. Because turbulence phenomena are associated with singular multifractal behavior (e.g., Sreenivasan [11]), space-filling fractal interpolating functions provide an unexpected bridge from *disorder to order*. Surprisingly, the opposite behaviors given by turbulence and the bell (e.g., diffusion) appear as the two sides (projections) of the same infinite attractor set, a wire that "filters" (transforms) any diffuse measure (over z) into the ordered bell [over the (x, y) plane]. To emphasize the relevance of this result, it should be added that the filtering of singular diffuse measures is attained only in the limiting space-filling case, as the usage of other fractal interpolating functions transforms disordered sets (over one dimension) into other disordered sets (over two dimensions) [12].

The following conditions guarantee the existence of a bivariate Gaussian over (x, y) (horizontal) from any parent diffuse measure in z (vertical) [4,12]:

1. the magnitude of all scalings $r_n^{(i)}$ tends to the limiting value of one, and
2. the rotations on each map satisfy $\theta_n^{(1)} = \theta_n^{(2)} + k\pi$, for any integer k.

These requisites ensure the convergence of the iteration procedure while driving the fractal dimension of the resulting wire toward three. Even though the construction implies a central limit theorem, these results are novel, as the relevant variates are not only depen-

FIGURE 2

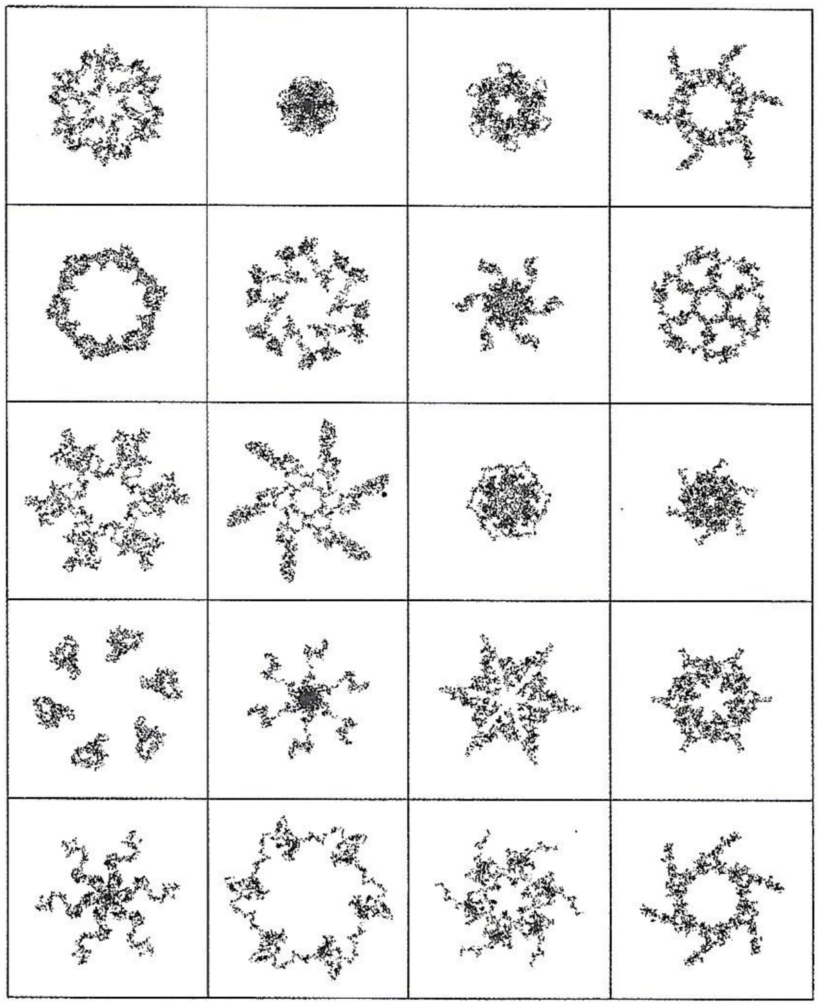

Sequential transient patterns inside the bell (left to right and bottom to top). Data: {(0, 0, 0), (1, 1, ½), (0, 0, 1)}. Scalings: $r_1^{(1)} = r_1^{(2)} = r_2^{(1)} = r_2^{(2)} = 0.9999$. Rotations: $\theta_1^{(1)} = \theta_1^{(2)} = 2\pi/3$, $\theta_2^{(1)} = \theta_2^{(2)} = \pi/3$. The iterations path is defined using pseudo-random numbers routine *ran1* [13] with –577 as seed and such that w_1 (in green) and w_2 (in red) are used, respectively, 70 and 30% of the time, defining a binomial multifractal measure over z. Iterations are started at (1, 1, ½) and each frame contains 4000 dots [in (x, y)].

dent, but also nonidentically distributed and unbounded [8].

DECOMPOSITION OF THE BIVARIATE GAUSSIAN DISTRIBUTION

In practice, many points within a wire need to be gathered in order to arrive at a bell. When more than, say, 15 million points are counted, close approximations of bivariate Gaussians are obtained when the magnitude of all scalings $r_n^{(i)}$ is close to the limiting value of 1, say 0.9999. When all rotations $\theta_n^{(i)}$ are synchronized, such that their maximum common divisor (modulus 2π) divides 2π, sequential transient symmetric patterns having arbitrary m-fold symmetry decompose circular bells [2]. As illustrated in Figure 2, these sets are obtained when the (x, y) coordinates of successively acquired points on a nearly space-filling attractor are plotted (just dropping the z component) in sequential groups containing few thousand dots at a time. They yield a value of m which, depending on sign combinations on the scaling parameters, is the aforementioned maximum common divisor, or half or twice of such a value [2].

Even though biased coins aided by pseudo-random numbers may naturally be used to specify a suitable iteration path, it is relevant to realize that the geometric sets decomposing the bell are, at the end, *deterministic designs* that lie hidden *inside the bell.* These designs represent "alternative universe," which strongly depend on the actual path of iterations traveled. Invariably, however, they provide striking crystalline kaleidoscopic patterns having unpredictable dynamics [2], which by varying data points, free parameters, and iteration paths, define great many sets. Altogether, they expound gigantic jigsaw puzzles of infinite varieties, whose pieces remarkably interlock to yield bells, suggesting that inside the bell there is *hidden order in chance* [2].

It is worth remarking, as already mentioned regarding the filtering of diffuse measures into bells, that it is near the Gaussian limit, when all scalings have magnitudes tending to 1, and only near such a limit, where exotic behavior is found. In fact, if these parameters are all sufficiently small (say, <0.99 in magnitude) evolutions that parallel the one given in Figure 2 become very predictable, as all sequential patterns, e.g., with 10,000 dots, give basically the same approximation of a unique and noncrystalline attractor [2].

DNA's ROSETTE AND THE BELL

The designs discovered inside the bell have a wide variety of shapes and some of them have striking similarity with natural patterns. They include a host of rosettes encompassing, among others, snow crystals and biochemical units

FIGURE 3

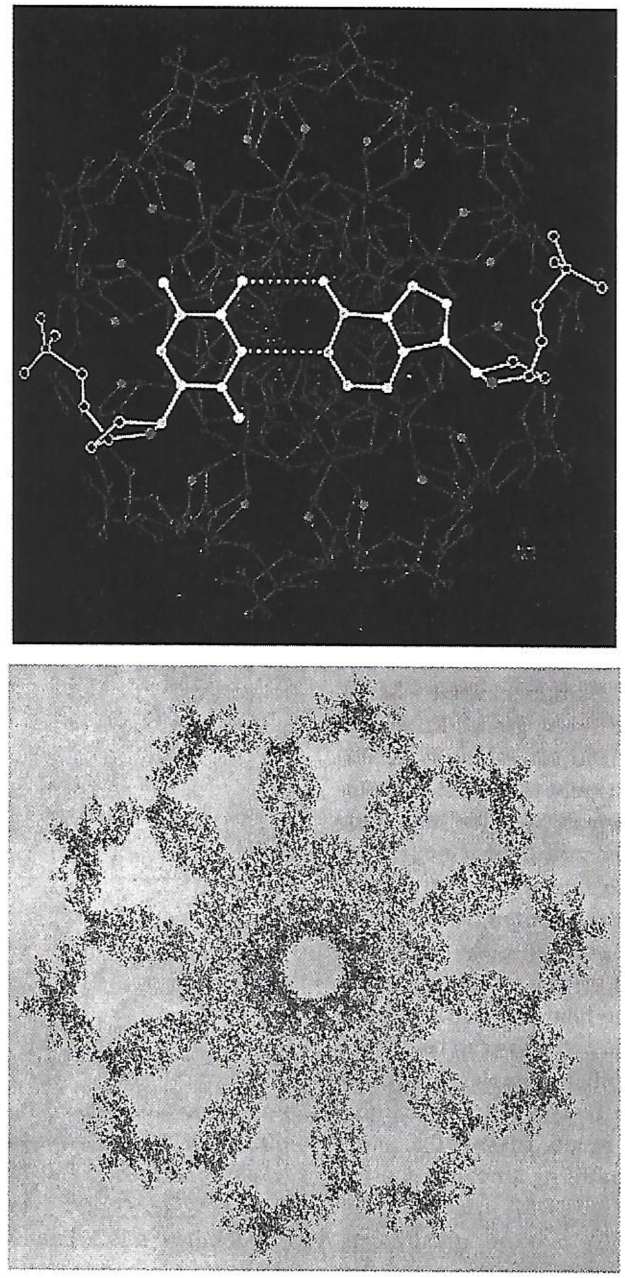

The planar structure of B-DNA (top) [1] and a close approximation as found inside the bell (bottom). Data: {(0, 0, 0), (1, 1, ½), (0, 0, 1)}. Scalings: $-r_1^{(1)} = r_1^{(2)} = r_2^{(1)} = r_2^{(2)} = 0.99999999999$. Rotations: $\theta_1^{(1)} = \theta_1^{(2)} = \theta_2^{(1)} = \theta_2^{(2)} = \pi/5$. The iterations path is defined interactively pasting pseudo-random numbers so that sequential points land on a template of the rosette. For details, see text.

such as viruses, proteins, and bacteria [14].

As shown in Figure 3, a suitable approximation of life's 10-fold B-DNA rosette may be found inside the bell via the usage of two simple affine mappings that are iterated according to an interactively defined pathway whose projected points fill up a template of the rosette. Specifically, the pattern inside the bell portrayed in Figure 3 is found pasting together several groups of 500 "tosses" each, as generated via pseudorandom numbers routine *ran1* [13], selecting a suitable group of tosses among 100 groups per seed, as follows: seed −4668, group 48; seed −798, group 44; seed −367, groups 46, 90, 19, 27, 54, 69, 100, 7, 46, 51, 3, 22, 73, 7, 36, 31, 28, 29, 15, 3, 6, 12, 8, 23, 46, 19, 55, 9, 86, 47, 66, and 77; seed −1675, group 54; seed −2678, groups 21, 84, 97, 64, 30, 76, 26, and 43; seed −337, groups 38, 30, 11, 31, 22, 81, 28, 23, and 22; seed −6715, groups 60 and 83; seed −1212, group 99; seed −3026, group 16; seed −1697, groups 27 and 83; seed −269, groups 80, 75, 70, 45, 51, 59, 91, 28, and 42; seed −154, group 9; seed −672, groups 99, 21, 73, 29, and 74; seed −1662, groups 21, 2, 16, 86, and 31; seed −261157, group 38; seed −94477, groups 22 and 60; seed −153, group 95; seed −64100, group 9; seed −126, groups 92 and 83. At the end, the set contains 42,500 nodes and excludes the first two groups in order to recreate the inner hole in the rosette.

As may be seen, the most relevant structure of the DNA template is nicely captured by projecting the sequential dots that sample the graph of a deterministic space-filling wire. Even though other iteration pathways can be defined to produce other suitable approximations of the template (not included here), these results suggest that other symmetric patterns (including other renderings of life's DNA rosette, e.g., Arnott et al. [15]) may be literally concealed as pieces of gigantic puzzles that are components of the circular bell, in a fashion that has a rather minimal computational complexity.

As arbitrary (pseudo-random) iterations of simple affine mappings yield beautiful kaleidoscopes, it becomes natural to ask if the sequences of digits making up the expansions of irrational numbers may encode relevant patterns inside circular bells. In this spirit, Figure 4 presents some examples of what the bell contains when the binary expansion of the number π sets up iterations between two mappings, for a space-filling wire that results in sets with 10-fold symmetry.

As may be seen, the digits of π do provide not only interesting patterns but also pertinent sets, such as the second one that is made up of 20,000 dots and is shown enlarged in Figure 5, that gives a topologically correct approximation of the projection of life's B-DNA, as already shown in Figure 3. Notice the appearance of rings and spokes in the real and generated patterns that leads to an unforeseen relation between the geometric structure of life and the binary digits of π, through the bell (albeit an approximation of a frozen picture over two dimensions). This intriguing linkage insinuates an unexpected avenue for finding "meaning" in the intrinsic "randomness" in π and leads us to wonder what else could its binary expansion (or others) may encode inside the bell (or others) in two and in higher dimensions.

A preliminary analysis of the first 100,000 binary digits of the numbers $\sqrt{2}$ and e reveals that they do not encode, either every 10,000 or 20,000 dots, the B-DNA rosette while employing the generic set of interpolating points used in Figure 4. These results clearly do not preclude the existence of such a shape later on or via alternative wires that pass by other points and rather invite us to further study the mysteries, of arbi-

FIGURE 4

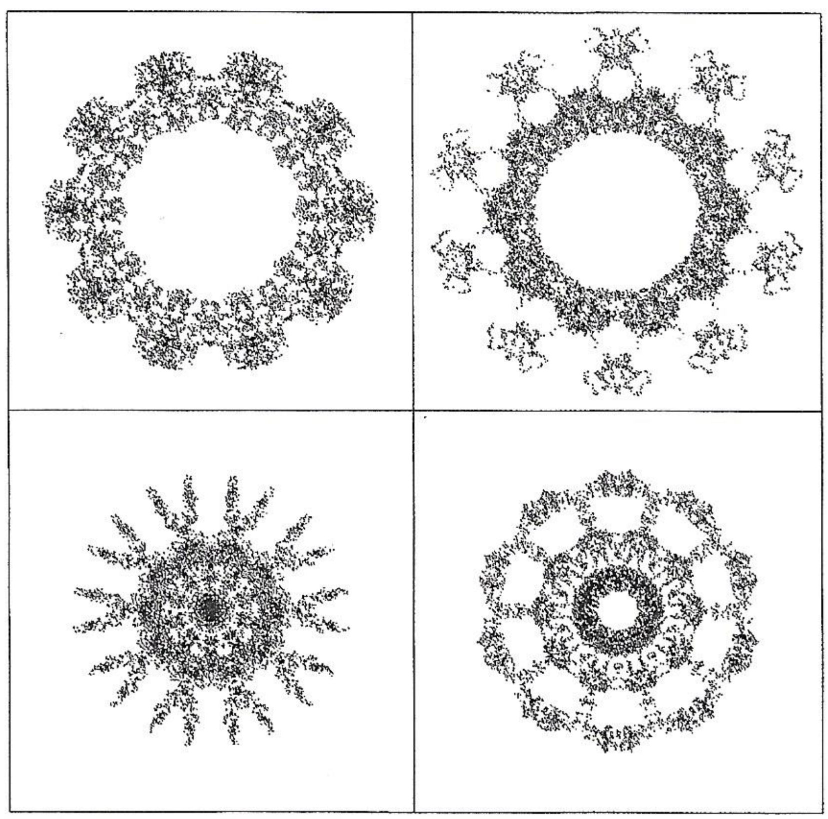

Sequential transient patterns inside the bell (left to right and bottom to top). Data: {(0, 0, 0), (1, 1, ½), (0, 0, 1)}. Scalings: $r_1^{(1)} = -r_1^{(2)} = r_2^{(1)} = r_2^{(2)} = 0.99999999$. Rotations: $\theta_1^{(1)} = \theta_1^{(2)} = 6\pi/5$, $\theta_2^{(1)} = \theta_2^{(2)} = \pi/5$. The iterations path is defined using the binary expansion of π, starting at (1, 1, ½) and plotting 20,000 dots per frame.

FIGURE 5

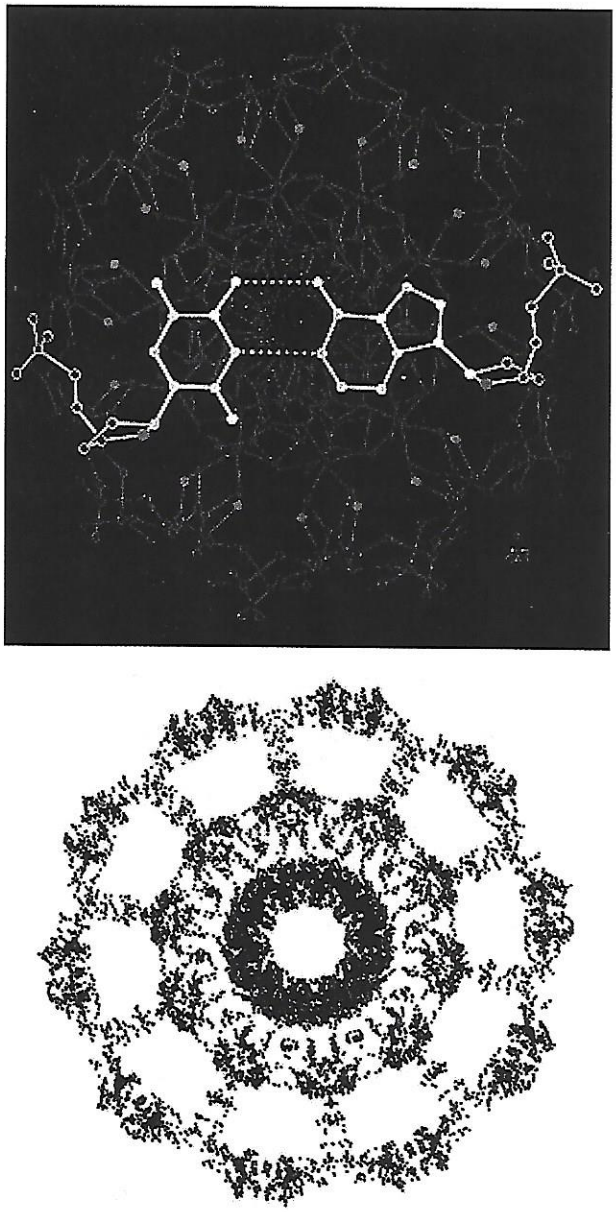

The planar structure of B-DNA (top) [1] and a topologically correct rendering as found inside the bell via the binary digits of π (bottom).

trary symmetries, which are encoded in the bell via such key numbers and others. For as may be appreciated, a set that at the end is a "simple wire" may code via one (or many) irrational number(s) a great many relevant shapes, in a manner that boggles the mind.

Although the findings in Figure 4 may be just a coincidence, the results portrayed in Figure 3 give us a glimpse at how likely it is to find the rosette via iterations, as follows. If one counts the number of cases that land inside the template used in Figure 3 and follows such a process stage by stage, i.e., in groups of 500, and if one assumes that such numbers are representative of any other possible path, one may find a probability for the rosette via their multiplication as 100, 3, 6, 9, 24, 11, 22, 49, 22, 25, 35, 62, 41, 63, 61, 4, 65, 84, 81, 82, 64, 89, 77, 91, 81, 84, 27, 65, 81, 34, 45, 61, 56, 52, 50, 49, 18, 47, 21, 18, 34, 52, 21, 40, 41, 52, 44, 14, 43, 54, 49, 19, 7, 13, 5, 21, 7, 5, 6, 10, 1, 4, 13, 10, 6, 10, 18, 5, 25, 1, 8, 13, 15, 8, 10, 17, 11, 9, 10, 12, 8, 7, 14, 10, and 3 (each divided by 100) to yield 3.64×10^{-59}. If the average acceptance probability for such an exercise, i.e., 0.32, is used to model the 40 groups of 500 points making up the graph in Figure 5, one gets another estimate for the probability of the DNA rosette as $(0.32)^{40}$ or 1.61×10^{-20}.

As there is an extremely large number of possible iteration scenarios inside the bell (i.e., in powers of 2, yielding $2^{40,000}$ alternatives when considering the first two patterns in Figure 4) and as added richness is obtained by varying the wire's interpolating points, finding the actual probability that the DNA rosette appears is, at the end, quite difficult. But the probability appears to be low, for if, say, just the 10,000th binary digit of π flipped from 1 to 0, then the rosette shown in Figure 4 no longer appears.

CONCLUSIONS AND FINAL REMARKS

In consonance with modern work in nonlinear dynamics, this work stresses that usage of simple mechanisms and the concept of projections may be central to understand complexity [14,16]. Because the appearance of patterns inside the bell evokes the concept of "emergence of order at the edge of chaos" [17] and because these sets arise only when the underlying wire fills up space, the ideas herein may be termed as *"emergence of order at the plenitude of dimension."*

As this work presents intriguing new results, it also raises some important questions. Why is the DNA rosette (and other natural patterns) found inside the bell? Is there a way to harmonize the existence of biochemical patterns inside the bell with observed organizational principles in nature? Could these findings be useful to further understand natural pattern formation and, in particular, the structure of life?

Even though symmetric patterns similar to those reported herein may be generated via nonlinear approaches that do not necessarily lead to the bell (e.g., Zaslavsky [18]), it is envisioned that the inherent structure of generalized central limit theorems, as implied by wires in higher dimensions or by other space-filling sets found via non-affine mappings, may be of relevance to study the aforementioned questions.

ACKNOWLEDGMENTS

The author is grateful for the equipment provided by Pacific Telesis in order to study what is inside the bell. The hard work of Nelson Obregón, Oscar Robayo, Demiray Simsek, and Marta G. Puente, and the continuous encouragement of Akin Orhun and Stephen Grattan are gladly acknowledged. The comments of Stephen Bennett and Bellie Sivakumar are gratefully appreciated. This work is dedicated to Jacobo Goldstein, an esteemed teacher who first introduced me to the beautiful bell.

REFERENCES

1. Voet, D.; Voet, J.G. Biochemistry; New York, John Wiley & Sons, 1995.
2. Puente, C.E. Fractals 1997, 5, 47.
3. Puente, C.E. Phys Lett A 1992, 161, 441.
4. Puente, C.E.; Klebanoff, A. Fractals 1994, 2, 65.
5. Barnsley, M.F. Constr Approx 1986, 2, 303.
6. Barnsley, M.F. Fractals everywhere; Boston, Academic Press, 1988.
7. Elton, J. J Erg Th Dyn Sys 1987, 7, 481.
8. Puente, C.E.; López, M.M.; Pinzón, J.E.; Angulo, J.M. Adv Appl Prob 1996, 28, 500.
9. Mandelbrot, B.B. In: Scholz, C.H.; Mandelbrot, B.B. (eds), Fractals in geophysics; Basel, Birkhauser, 1989, 1–42.
10. Feder, J. Fractals; New York, Plenum, 1988.
11. Sreenivasan, K.R. Annu Rev Fluid Mech 1991, 23, 539.
12. Puente, C.E. In: Dimitrakopoulos, R. ed.), Geostatistics for the next century; Dordrecht, Kluwer Academic Publishers, 1994, 476–481.
13. Press, W.H.; Flannery, B.P.; Teukolsky, S.A.; Vetterling, W.T. Numerical Recipes; Cambridge, Cambridge University Press, 1989.
14. Puente, C.E.; Obregón, N.; Robayo, O.; Puente, M.G.; Simsek, D. Fractals 1999, 7, 387.
15. Arnott, S.; Chandrasekaran, R.; Banerjee, A.K.; He, R.; Walker, J.K. J Biomol Stra Dyn 1983, 1, 437.
16. Puente, C.E. (2001). Treasures inside the bell: Hidden order in chance. World Scientific Publishing Company (In preparation). A related web site is under construction at http://gul.ucdavis.edu/belltreasures.
17. Kauffman, S. The origins of order; New York, Oxford University Press, 1993.
18. Zaslavsky, G.M. Physics of Chaos in Hamiltonian Systems; London, Imperial College Press, 1998.